CHEMICAL ENGINEERING TRANSACTIONS
VOL. 103, 2023
A publication of AIDIC
The Italian Association of Chemical Engineering
Online at www.cetjournal.it
Guest Editors: Petar S. Varbanov, Panos Seferlis, Yee Van Fan, Athanasios Papadopoulos

ISBN 979-12-81206-02-1; **ISSN** 2283-9216
DOI: 10.3303/CET23103085

Modelling and Evaluation of CO_2-based Electrothermal Energy Storage System

Alexios-Spyridon Kyriakides[a,*], Aristeidis Stoikos[a], Dimitrios Trigkas[a,b], Georgios Gravanis[a], Ioannis N. Tsimpanogiannis[a], Simira Papadopoulou[a,b], Spyros Voutetakis[a]

[a]Chemical Process and Energy Resources Institute, Centre for Research and Technology-Hellas, 60361, 57001 Thermi, Thessaloniki, Greece
[b]Department of Industrial Engineering and Management, International Hellenic University, 57001 Thessaloniki, Greece
alexkyr@certh.gr

The use of renewable energy sources as a solution to the energy dependency on fossil fuels requires innovative solutions to the issue of energy storage. Among the solutions suggested in the literature, electrothermal energy storage comprised of a heat pump and a heat engine using transcritical CO_2 cycles, water as a thermal energy storage (TES) fluid to store sensible heat and ice as a cold storage medium to store latent heat, appears promising. In this paper, a steady state mathematical model of the system is developed using Aspen Plus V11, validated and compared against results available in the literature. The validated model's performance is then studied utilizing parametric sensitivity analysis by exploring the effect of different parameters on multiple efficiency metrics, with the best case achieving improvement on the round-trip efficiency ($\eta_{R\text{-}T}$) of 7.64 %. The hydraulic turbine inlet temperature and the heat engine minimum pressure are found to contribute the most to the $\eta_{R\text{-}T}$ improvement, with the minimum pressure being the one that can be further decreased by using cold TES mediums with lower freezing points. Finally, the effect of alternative cold TES mediums (with lower freezing temperature than ice) on the performance of the system is evaluated. It was concluded, that the $\eta_{R\text{-}T}$ of the model decreases as the freezing temperature declines, from 46.90 % at 0 °C to 44.90 % at -20.19 °C. As a result, no benefit related to the $\eta_{R\text{-}T}$ of the model can be deduced by choosing cold TES mediums with lower freezing p than ice.

1. Introduction

All around the world, governments are taking action to mitigate the energy dependence on fossil fuels, which have a negative impact both on electricity prices and CO_2 emissions (International Energy Agency, 2022). According to the States Policies Scenario (STEPS), created by the International Energy Agency (2022), which is based on the actual guidelines being implemented by several governments, fossil fuels as a percentage of the total energy composition will drop from 80 % today to less than 75 % in 2030 and to approximately 60 % in 2050. At the same time, the increase of 1 %/y in energy demand until 2030 according to the same report (International Energy Agency, 2022), is satisfied mostly through the use of renewable sources. As a result, the importance of renewable energy sources is becoming more prominent.

One of the main challenges facing the adoption of renewable energy sources like solar and wind, is the mismatch between demand and readily available supply (Boretti and Castellato, 2022). A solution to this issue is using energy storage (ES) to store the excess energy and use it on demand (Fernandez et al., 2019). Koohi-Fayegh and Rosen (2020) analysed different types of ES, with pumped hydro and compressed air being two of the more developed, which are also better suited for large scale ES, both presenting however geographical limitations. Ortenero and Tan (2021), deployed the multiple attribute decision-making method VIKOR to grade different ES methods and concluded that for limited space areas electrochemical methods like Li-ion batteries are the optimal choice, their use, however, requires a comprehensive safety supervision mechanism (Marlair et al., 2022). Another ES method appearing in the literature, is electrothermal energy storage (EES). Mercangöz et al. (2012)

Paper Received: 15 April 2023; Revised: 13 May 2023; Accepted: 30 May 2023
Please cite this article as: Kyriakides A.-S., Stoikos A., Trigkas D., Gravanis G., Tsimpanogiannis I.N., Papadopoulou S., Voutetakis S., 2023, Modelling and Evaluation of CO_2-based Electrothermal Energy Storage System, Chemical Engineering Transactions, 103, 505-510 DOI:10.3303/CET23103085

mentioned that EES, by itself, as an idea originated in the patent by Cahn (1978). In the same work, the authors introduced the idea of EES employing a heat pump (HP) and a heat engine (HE) with transcritical CO_2 (TCO_2) as a working fluid (WF), water as a secondary fluid to store heat and ice as a cold storage medium. Morandin et al. (2012), developed an EES model and optimised it through the heat integration of TCO_2 cycles. Fernandez et al., (2019) analyzed the behaviour of different EES configurations, using TCO_2 as a WF, including a case where supplementary heat from solar sources is added to the cycles. Finally, Carro et al. (2022) presented an alternative design to EES in terms of CO_2 capture and storage within underground geological structures. Although the ES and EES systems are examined in literature, most studies focus on alternative designs (e.g., include geological storage) or heat integration. However, the effect of different storage mediums and their corresponding properties (e.g., freezing point) have not been examined in the combined EES system.
In the present work, the effect of alternative TES medium options on the system's performance is evaluated. As a result, a steady state mathematical model for the EES system based on the BEES (Basic Electrothermal Energy Storage) system developed by Carro et al. (2022) is developed and validated, before being utilized in parametric analysis studies aiming to improve the overall system's performance. In section 2, the overall mathematical model is presented. In section 3, the model is validated against simulation results presented by Carro et al. (2022) and parametric sensitivity analysis is employed, aiming to improve the performance of the overall system. In section 4, the results are discussed in comparison with those of the BEES system as well as the ones generated by the employment of different TES configurations. Finally, in section 5 the most important conclusions along suggestions for future work are presented.

2. Mathematical model

2.1 Process description

The overall system is composed of two thermodynamic cycles (HP and HE). Excess electricity produced from renewable energy sources (e.g., solar or wind) is converted, during low demand periods, and stored into thermal energy through the use of a charge cycle (HP). A discharge cycle (HE) is then used to convert the thermal energy back into electricity during peak demand hours. The steady state mathematical model was created using the software Aspen Plus V11, the flowsheet of which is shown in Figure 1.

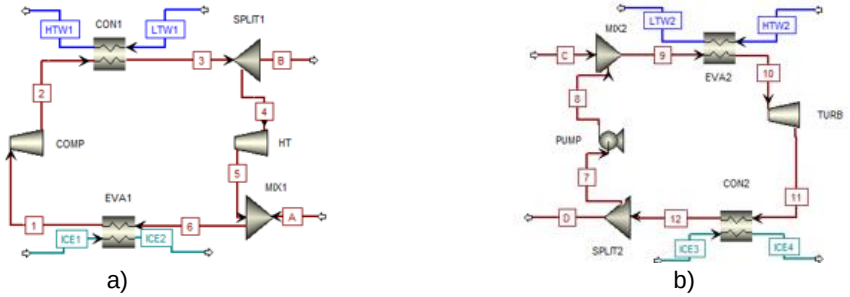

Figure 1: Electrothermal energy storage system flowsheet configuration: a) charge and b) discharge cycles.

Regarding the WF, CO_2 is considered a good option (Mercangöz et al., 2012), mainly due to its low critical point (31.1 °C, 73.8 bar) and good thermal properties. It is also more environmentally friendly than other WF, it is not flammable nor toxic. Regarding the secondary fluid used to store sensible heat, water is considered significantly better than other fluids, since it is characterized by a higher heat capacity, on top of being cheaper and more readily available. Ice is chosen as a cold TES medium since it offers the option of storing both sensible and latent heat at low cost (Carro et al., 2022) while increasing the overall performance due to larger temperature differences compared to water in ambient temperatures (Mercangöz et al., 2012).
In the **charge cycle** (Figure 1a), CO_2 is compressed isentropically (COMP) to reach its supercritical state and maximum temperature, using the electricity generated by the renewable sources. Then, it is condensed isobarically at a heat exchanger (CON1), releasing sensible heat to the water (secondary fluid, hot TES medium). Following that, the CO_2 expands isentropically through a hydraulic turbine (HT), producing work which can be used to contribute to the net-work cycle requirements. Finally, the CO_2 evaporates isobarically through a heat exchanger (EVA1) absorbing latent heat from the ice. In the discharge cycle (Figure 1b), CO_2 in liquid form is compressed isentropically (PUMP). It then evaporates through a heat exchanger isobarically (EVA2), absorbing sensible heat from the water which is being stored in the hot storage tank. Having reached its maximum temperature, the CO_2 expands through a turbine isentropically (TURB), generating work which is used to generate electricity for the network. Finally, it is condensed through a heat exchanger isobarically (CON2), releasing latent heat to the ice.

2.2 Model assumptions and thermodynamic properties

REFPROP method, version 10.0.0.02., developed by the National Institute of Standards and Technology (NIST) which utilizes the Span-Wagner equation of state (EoS) (Aspen Technology Inc., 1981-2019), is used to calculate the thermodynamic properties of pure CO_2. IAPWS-95 EoS is used to calculate the thermodynamic properties of pure water. The following model assumptions were made:

- CO_2 is considered pure, without any impurities
- The kinetic and potential energy changes are considered insignificant
- The compressor, hydraulic turbine, pump and turbine are considered to operate adiabatically
- The flows through the heat exchangers are considered counter-current

Each cycle operates between a maximum and a minimum pressure. In order to maximize both cycles' performance and to fully utilize the stored thermal energy, minimum and maximum pressures are selected based on the cold and hot TES conditions. More specifically, low pressure must be such that CO_2 is near its phase change point (saturation line) at the respective heat exchanger temperature (either EVA1 or CON2). Given that ice is selected as the cold TES medium, operating at 1 bar and 0 °C, minimum pressure is chosen to be equal to 34.85 bar (Carro et al., 2022). At this pressure CO_2 changes phase at 0 °C. Similarly, high pressure must be such that CO_2 is at its supercritical state at the respective heat exchanger temperature (CON1 and EVA2). An additional constraint at this point is the possible turbomachinery limitations and material cost increase at higher pressures. Also, given that water is selected as the hot TES medium, operating at 8 bar (boiling point at 170 °C), and since water evaporation in the TES tank is undesirable (Carro et al., 2022), high pressure is chosen to be up to 200 bar. At this pressure, CO_2 reaches maximum temperatures below 170 °C.

3. Implementation details

3.1 Model validation

The validation of the current mathematical model is performed against simulation results presented by Carro et al. (2022). The base case model conditions, presented in Table 1, are chosen based on Carro et al. (2022).

Table 1: Base case model parameters

Parameter	Equipment	Value	Unit
Isentropic efficiencies	Compressor/Pump	0.86/0.85	
	Hydraulic turbine/Turbine	0.85/0.88	
Pinch point	Heat exchangers	4	°C
Net-work input	Charge cycle	1,000	kW
Charge and discharge cycle pressures ($P_{HP,Low}$/$P_{HP,High}$) - ($P_{HE,Low}$ /$P_{HE,High}$)		30/200 - 40/190	bar
Charge and discharge cycle flowrate ($\dot{m}_{CO2,char/dis}$)		12.2/23.9	kg/s
Charge and discharge cycle water flowrate ($\dot{m}_{H2O,char/dis}$)		6.4/13.2	kg/s
Low temperature water temperature (T_{LTW1}/T_{LTW2})		23/23.1	°C
Charge and discharge cycle ice flowrate ($\dot{m}_{ice,char/dis}$)		6.3/16.1	kg/s
Low and high temperature of ice ($T_{ice,low}$/$T_{ice,high}$)		-1.5/1.3	°C
Charging hours water/ice (h_{char})		10	h

The model is evaluated using the $\eta_{R\text{-}T}$ of the system ($\eta_{R\text{-}T}=\left(\left(W_T\text{-}W_{Pump}\right)/(W_C\text{-}W_{HT})\right)\times(h_{dis}/h_{char})$) and the individual cycle efficiencies, namely of the charge ($\eta_{HP}=\left(Q_{HS,HP}+Q_{CS,HP}\right)/(W_C\text{-}W_{HT})$) and discharge cycle ($\eta_{HE}=\left(W_T\text{-}W_{Pump}\right)/\left(Q_{HS,HE}+Q_{CS,HE}\right)$). W_T and W_{HT} are the power generated by the turbine and the hydraulic turbine in kW, while W_C and W_{Pump} are the required power by the compressor and the pump in kW. Similarly, $Q_{HS,HP}$ and $Q_{HS,HE}$ are the sensible heat stored and released to and from the hot TES unit in kW, while $Q_{CS,HP}$ and $Q_{CS,HE}$ are the latent heat released and stored from and to the cold storage tank in kW. Finally, h_{char} are the hours of operation of the charge cycle (charging) and h_{dis} are the hours of operation of the discharge cycle (discharging).

3.2 Sensitivity analysis

Having established the BEES model validity in the previous section (see also results section), the main parameters that contribute to the $\eta_{R\text{-}T}$ are explored through parametric sensitivity analysis using Aspen Plus V11 and the fundamental thermodynamic principles.

Maximum working pressures of the charge cycle (P_2=P_3, $P_{HP,High}$) and discharge cycle (P_9=P_{10}, $P_{HE,High}$) are chosen in order to evaluate their effect on the system's performance, through the sensitivity analysis. For a fixed minimum pressure of the charge cycle (P_1=P_6, $P_{HP,Low}$) and a fixed temperature at the hydraulic turbine inlet,

increasing the $P_{HP,High}$ leads to higher maximum temperature of the WF and sensible heat at higher temperature can be released. This leads to a higher maximum temperature of the hot TES water assuming fixed lower temperature water. In turn that will lead to higher maximum temperature of the WF of the discharge cycle which results to higher turbine work output or discharge periods. It is important to mention here that two constraints are employed during the simulation of the cycles. The first one is related to the net-work input of the charge cycle (1,000 kW), as the one selected by Carro et al. (2022), and is employed to enable comparability throughout the results. The second one is related to the net-work output of the discharge cycle (-1,000 kW), and is employed to alter the discharge period duration instead of the capacity of the cycle. Both constraints are satisfied by changing the respective cycle's WF mass flow rate. For the maximum pressures, the ranges that were explored were between 160 and 220 bar with the upper limit being set based on the factors mentioned in section 2.2. All other model parameters are chosen based on the model of Carro et al. (2022), as shown in Table 1, except for two parameters, namely T_3 and the minimum pressure of the discharge cycle (P_{11}=$P_{12,}$ $P_{HE,Low}$). Temperature T_3 is fixed at 32 °C since it offers the maximum temperature difference on CON1 heat exchanger while maintaining CO_2 at supercritical conditions. $P_{HE,Low}$ is fixed at 37 bar since that is the pressure that offers the maximum pressure differences on the turbine for variable maximum pressure while also generating temperatures that comply with the pinch point value of 4 °C.

4. Simulation results

4.1 Model validation

In Table 2, a comparison is made between the base case simulation results and results presented by Carro et al. (2022) where it is shown that the temperatures at the four points of each of the charge and discharge cycles are almost identical. The same conclusion is shown for the net-work input and output for each model. Overall, it is clearly visible that, based on individual cycle and overall system efficiencies, base case model results are in excellent agreement with the reference model. More specifically, η_{HP} is exactly the same, while a small deviation is observed in η_{HE} and $\eta_{R\text{-}T}$.

Table 2: Simulation and sensitivity analysis results. Comparison between base case and best case

Parameter	Carro et al. (2022)	Base case model	Best case sensitivity analysis	Unit
Net-work input/output	1,000/1,000	996.69/998.37	999.98/1,000	kW
T_1/T_6	-5.5/-5.55	-5.55/-5.55	-5.55/-5.55	°C
T_2/T_{10}	157.8/136.8	157.76/136.47	164.37/156.37	°C
T_3	40	40	32	°C
T_9	19.1	19.37	18.07	°C
T_{11}	14.4	14.13	14.71	°C
T_{12}	5.3	5.29	2.27	°C
η_{HP}/η_{HE}	5.3/0.08	5.3/0.083	5.45/0.095	
Discharge hours – water/ice	4.82/3.91	4.85/3.92	5.61/4.69	h
Non-used energy on hot TES tank	23.26	23.72	19.61	%
$\eta_{R\text{-}T}$	39.1	39.26	46.90	%

4.2 Sensitivity analysis results and cold TES medium effect on performance

In Table 2, results of the best case (highest $\eta_{R\text{-}T}$), as found through the sensitivity analysis, are presented in comparison with the base case model results and results presented by Carro et al. (2022). The results show that the best case $\eta_{R\text{-}T}$ has risen by 7.64 %. This result corresponds to a $P_{HP,High}$ of 214 and $P_{HE,High}$ of 220 bar. At the same time, the non-utilised thermal energy left in the hot storage tank has dropped from 23.72 % to 19.61 % which is explained by the increase in the discharge hours of the cycle to the cold storage. Finally, the other two indicators are also improved, the η_{HP} from 5.3 to 5.45 and the η_{HE} from 0.083 to 0.095.

In Figures 2a and 2b, a comparison between the best case and base case model results is presented, based on the *T-s* diagrams. As it is visible in combination with the results from Table 2, for the best case results, net-work input and output have increased however they remain close in value. This leads to the conclusion that the increase in the $\eta_{R\text{-}T}$ is mainly due to the increase to the discharge hours of the ice. T_1 and T_6 remain the same since the pressure at those points for both simulations remains stable at 30 bar while T_2 and T_{11} see an increase due to the increase in the $P_{HP,High}$. T_{10} has increased due to the increase of T_2 and the subsequent increase of T_{HTW1}/T_{HTW2}. Finally, T_9 and T_{12} see a small decrease due to the smaller value of the $P_{HE,Low}$.

In Figure 3a, the effect that both sensitivity analysis variables ($P_{HP,High}/P_{HE,High}$) have on the $\eta_{R\text{-}T}$, are presented. Higher $P_{HE,High}$ results in increased $\eta_{R\text{-}T}$, with variable slope, that is higher increase rate is observed for higher $P_{HP,High}$. At the same time, higher values for $P_{HP,High}$ lead to lower values of $\eta_{R\text{-}T}$ with variable slope, that is less

decrease rate is observed for higher $P_{HE,High}$. In fact, the slope marginally reverses, at the highest values of $P_{HE,High}$. These results lead to the conclusion that the highest values of η_{R-T} are observed when $P_{HP,High}$ and $P_{HE,High}$ have their highest values with $P_{HP,High}$ having the least impact of the two. Another comment that can be made is that even for the same $P_{HP,High}$ and $P_{HE,High}$ as the ones used by Carro et al. (2022), 200/190 bar, the η_{R-T} increases to 46.36 %. This is attributed to the changes on the two fixed variables, T_3 and $P_{HE,Low}$, that had a significant impact on the η_{R-T}. Of the two, $P_{HE,Low}$ could be further decreased, if the cold TES medium had a lower freezing point.

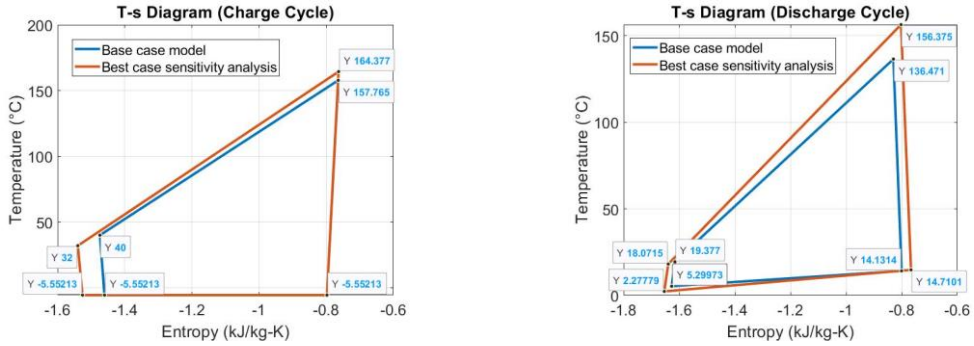

a) b)

Figure 2: T-s diagram for a) charge and b) discharge cycles. Best case against reference model

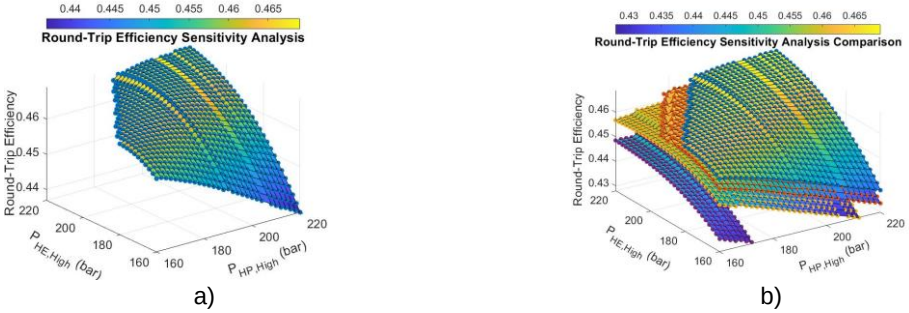

a) b)

Figure 3: Round-trip efficiency a) against sensitivity analysis variables ($P_{HP,High}$/$P_{HE,High}$) and b) comparison between models using cold TES medium with freezing points 0 °C (blue markers), -4.47 °C (red markers), -11.04 °C (orange markers) and -20.19 °C (purple markers)

Based on the above observation, an ethyl-alcohol water solution (ice slurry) was used, to see how the usage of a cold TES medium with a lower freezing point than ice might affect the performance of the model. Three solutions were tested with different freezing points. The data regarding concentration, ice mass concentration, freezing temperature and ice slurry temperature of the solutions were chosen from the study by Melinder and Granryd (2005) and are shown in Table 3.

Table 3: Ice slurry input data and results.

#	Additive w.t. % (kg additive/kg total)	Ice w.t. % (kg ice/kg total)	Freezing T (°C)	Ice slurry T (°C)	$P_{HP,Low}$ (bar)	$P_{HE,Low}$ (bar)	$P_{HP,High}$ (bar)	$P_{HE,High}$ (bar)	η_{HP}	η_{HE}	η_{R-T} (%)
1	0.1	0.22	-4.47	-6	26	33	202	220	5.16	0.100	46.51
2	0.2	0.06	-11.04	-12	22	29	194	220	4.82	0.107	45.99
3	0.3	0.05	-20.19	-22	16	23	168	220	4.41	0.116	44.90

$P_{HP,Low}$ *and* $P_{HE,Low}$ were selected for the temperature difference between the WF and the ice slurry on each cycle to be greater than 4 °C. For each solution, parametric sensitivity analysis was conducted as in section 3.2, with variable maximum pressures on each cycle ($P_{HP,High}$/$P_{HE,High}$). The results show, in Table 3, that the η_{R-T} decreases as the freezing temperature of the ice slurry decreases. The individual cycle efficiencies move in opposite directions with the η_{HP} decreasing and the η_{HE} increasing for declining freezing temperatures while the optimal $P_{HP,High}$ decreases and the one of the HE ($P_{HE,High}$) remains stable at 220 bar. The same conclusion can

be made in Figure 3b, where it is shown that for decreasing freezing temperatures, the surface curve of the η_{R-T} shifts to lower values. Based on the above results, in terms of the η_{R-T} of the model, there is no benefit in choosing ice slurries with lower freezing points than ice as cold TES medium.

5. Conclusion

A steady state mathematical model was developed to simulate an EES system and evaluate its performance for different operating conditions. The model was validated against literature reported results, generating near identical individual and η_{R-T} efficiencies, proving the validity of the model. Parametric sensitivity analysis was then used to evaluate the system's performance with $P_{HP,High}$ and $P_{HE,High}$ as sensitivity variables and T_3 and $P_{HE,Low}$ parameter values changed. As a result, for $P_{HP,High}$ and $P_{HE,High}$ equal to 214 and 220 bar, the η_{R-T} was improved by 7.64 %, up to 46.90 %, the non-utilised thermal energy left from 23.72 % to 19.61 %, the η_{HP} from 5.3 to 5.45 and the η_{HE} from 0.083 to 0.095. In general, it is observed that η_{R-T} rises, when $P_{HP,High}$ and $P_{HE,High}$ decreases and increases for fixed values of T_3 and $P_{HE,Low}$. Additionally, the $P_{HP,Low}$ and $P_{HE,Low}$ could be further decreased by using cold TES mediums with lower freezing point. Parametric sensitivity analysis was then used to evaluate the system's performance under progressively lower freezing points. The results indicate that in terms of η_{R-T}, there is no advantage on using such solutions since it declined from 46.90 % at 0 °C to 46.51 % at -4.47 °C, 45.99 % at -11.04 °C and 44.90 % at -20.19 °C. In future work we will analyze the limitation that the steady state modelling and analysis has on the evaluation of the η_{R-T} of the process by employing dynamic mathematical modelling when the charging/discharging of the TES tanks is conducted in dynamic manner, reaching the optimal temperatures gradually.

Acknowledgements

This research has received funding from the European Union HORIZON Europe project CEEGS-NOVEL CO2-BASED ELECTROTHERMAL ENERGY AND GEOLOGICAL STORAGE SYSTEM, under Grand Agreement Number: 101084376. Views and opinions expressed are however those of the author(s) only and do not necessarily reflect those of the European Union or CINEA. Neither the European Union nor the granting authority can be held responsible for them.

References

Aspen Technology Inc., 1981-2019, Aspen Plus V11 <www.aspentech.com/en/products/ engineering/aspen-plus> accessed 07.03.2023.

Boretti A., Castellato S., 2022, Lacking energy storage, and nuclear contribution, wind, and solar photovoltaic electricity is expensive and scarce, The Electricity Journal, 35, 107222.

Cahn R.P., 1978, Thermal energy storage by means of reversible heat pumping, United States Patent, 4,089,744, Millburn N.J., USA.

Carro A., Chacartegui R., Ortiz C., Carneiro J., Beccera J.A., 2022, Integration of energy storage systems based on transcritical CO_2: Concept of CO_2 based electrothermal energy and geological storage, Energy, 238, 121665.

Fernandez R., Chacartegui R., Beccera A., Calderon B., Carvalho M., 2019, Transcritical Carbon Dioxide Charge-Discharge Energy Storage with Integration of Solar Energy, Journal of Sustainable Development of Energy, Water and Environment Systems, 7(3), 444-465.

International Energy Agency, 2022, World Energy Outlook 2022 <www.iea.org/reports/world-energy-outlook-2022> accessed 05.03.2023.

Koohi-Fayegh S., Rosen M.A., 2020, A review of energy storage types, applications and recent developments, Journal of Energy Storage, 27, 101047.

Marlair G., Lecocq A., Bordes A., Christensen P., Truchot B., 2022, Key Learnings from Recent Lithium-ion Battery Incidents that have Impacted e-mobility and Energy Storage Fast Growing Market, Chemical Engineering Transactions, 90, 643-648.

Melinder Å., Granryd E., 2005, Using property values of aqueous solutions and ice to estimate ice concentrations and enthalpies of ice slurries, International Journal of Refrigeration, 28, 13-19.

Mercangöz M., Hemrle J., Kaufmann L., Z'Graggen A., Ohler C., 2012, Electrothermal energy storage with transcritical CO_2 cycles, Energy, 45, 407-415.

Morandin M., Maréchal F., Mercangöz M., Buchter F., 2012, Conceptual design of a thermo-electrical energy storage system based on heat integration of thermodynamic cycles – Part A: Methodology and base case, Energy, 45, 375-385.

Ortenero J.R., Tan R.R., 2021, Ranking Energy Storage Technologies with VIKOR, Chemical Engineering Transactions, 88, 151-156.